

# Thermodynamic properties of Al, Ni, NiAl, and Ni<sub>3</sub>Al from first-principles calculations

Y. Wang<sup>\*</sup>, Z.-K. Liu, L.-Q. Chen

*Department of Materials Science and Engineering, Pennsylvania State University, 305 Steidle Building, State College, University Park, PA 16802-5006, USA*

Received 10 October 2003; received in revised form 9 February 2004; accepted 11 February 2004  
Available online 12 March 2004

## Abstract

The thermodynamic properties of Al, Ni, NiAl, and Ni<sub>3</sub>Al were studied using the first-principles approach. The 0-K total energies are calculated using the ab initio plane wave pseudopotential method within the generalized gradient approximation. The contribution to the free energy from the lattice vibration was calculated using the phonon densities of states derived by means of the ab initio linear-response theory. The thermal electronic contribution to the free energy was obtained from the one-dimensional numerical integration over the electronic density of states. With the deduced Helmholtz free-energy, the thermal expansion and enthalpy as a function of temperature were calculated and compared with the experimental data. Our calculations show that the enthalpies of formation are slightly temperature dependent with a slope of  $-1.6$  J/mol/K for NiAl and  $-1.2$  J/mol/K for Ni<sub>3</sub>Al. For Ni, the inclusion of thermal electronic excitation results in a 10% increase in thermal expansion and 15% increase in enthalpy at 1600 K.

© 2004 Acta Materialia Inc. Published by Elsevier Ltd. All rights reserved.

*Keywords:* Nickel alloys; Aluminium alloys; Ab initio electron theory; Thermodynamics

## 1. Introduction

With the advances in computational methods and computer speed, the first-principles technique is becoming a powerful tool in understanding and predicting the structural and physical properties of a material. In the specific field of phase diagram and thermodynamic properties of alloys, one currently needs to calculate three additive contributions to the free energy, depending on the required accuracy and the complexity of studied system.

The first contribution to consider is the cold energy or the 0-K total energy. In this case, the atoms are kept fixed at their static lattice positions. Most of published works stop at this stage by various reasons, such as, the system is too complex and only qualitative results are

needed, the role of ionic vibration is weak, or just the 0-K energies of formation are needed, etc.

To calculate the structural and thermodynamic properties at finite temperatures, the contribution of lattice thermal vibration to the total free energy needs to be taken into account. Theoretically, the commonly accepted method is the lattice dynamics or phonon approach. In this approach, within the harmonic or quasiharmonic approximation, all thermodynamic formulas are strictly derived on the basis of statistical physics. One of the main advantages is that all the quantities needed for input to the phonon theory can be calculated by means of ab initio methods [1–6].

When temperature is increased, especially for cases when the electronic density of state at the Fermi level is high, the third contribution to be included is the thermal electronic contribution (TEC) to the free energy. In most of the previous works [3,5–10], TEC has been neglected. Although neglect of TEC may be acceptable at low temperatures, it can be very significant at high temperatures. Take Ni as an example, its coefficient of

<sup>\*</sup> Corresponding author. Tel.: +1-814-865-0389; fax: +1-814-865-2917.

E-mail address: [yuw3@psu.edu](mailto:yuw3@psu.edu) (Y. Wang).

electronic specific heat  $\gamma$  is 7.02 mJ/mol/K<sup>2</sup>. Therefore, for  $T = 1000$  K, its contribution to the specific heat is  $\gamma T = 7.02$  J/mol/K which is 28% of classical constant volume specific heat of 24.94 J/mol/K.

In this paper, employing the ab initio linear-response approach [11], we systematically studied the thermodynamic properties of Al, Ni, NiAl, and Ni<sub>3</sub>Al. Ni–Al is the base binary system for the technologically important Ni-base superalloys which have been extensively used as high-temperature materials for turbine blades in aircraft engines due to their low specific weight, high melting point, and good chemical stability. In particular, we investigated the phonon dispersion, the thermal expansion, and the enthalpy of formation of the alloys as a function of temperature. Special attention is given to the role played by the thermal electronic excitation in thermodynamic properties at high temperatures.

## 2. Theory

In a system with an averaged atomic volume  $V$  at temperature  $T$ , the Helmholtz free-energy  $F(V, T)$  can be approximated as

$$F(V, T) = E_c(V) + F_{\text{ph}}(V, T) + F_{\text{el}}(V, T), \quad (1)$$

where in the framework of ab initio calculations,  $E_c$  is the 0-K total energy.  $F_{\text{ph}}$  is the vibrational free energy of the lattice ions and under the quasi-harmonic approximation it is given by [2]

$$F_{\text{ph}}(V, T) = k_B T \sum_{\mathbf{q}} \sum_j \ln \left\{ 2 \sinh \left[ \frac{\hbar \omega_j(\mathbf{q}, V)}{2k_B T} \right] \right\}, \quad (2)$$

where  $\omega_j(\mathbf{q}, V)$  represents the frequency of the  $j$ th phonon mode at wave vector  $\mathbf{q}$ . When the magnetic contribution and the electron–phonon interactions are neglected, the TEC to the free energy  $F_{\text{el}}$  is obtained from the energy and entropy contributions, i.e.,  $E_{\text{el}} - TS_{\text{el}}$  [12]. The bare electronic entropy  $S_{\text{el}}$  takes the form

$$S_{\text{el}}(V, T) = -k_B \int n(\varepsilon, V) [f \ln f + (1 - f) \ln(1 - f)] d\varepsilon, \quad (3)$$

where  $n(\varepsilon, V)$  is the electronic density of states (DOS) with  $f$  being the Fermi distribution.

The energy  $E_{\text{el}}$  due to the electron excitations can be expressed as

$$E_{\text{el}}(V, T) = \int n(\varepsilon, V) f \varepsilon d\varepsilon - \int^{\varepsilon_F} n(\varepsilon, V) \varepsilon d\varepsilon, \quad (4)$$

where  $\varepsilon_F$  is the Fermi energy.

It should be mentioned that the configuration disordering at high temperatures was not considered in the present calculations due to the extreme complexity in treating this. This assumption is reasonable for the

stoichiometric NiAl and Ni<sub>3</sub>Al compounds, which have very limited configurational disordering even at temperature near their melting temperatures [13].

## 3. Calculation procedure

To calculate the 0-K total energy  $E_c$  in Eq. (1) and the phonon frequency  $\omega_j(\mathbf{q}, V)$  in Eq. (2), the plane-wave self-consistent field (PWSCF) method [11] based on the ab initio linear-response theory was employed. We adopt the Vanderbilt ultra-soft pseudopotential [14,15] with the generalized gradient approximation (GGA) [16] to the exchange–correlation functional. The electronic DOS  $n(\varepsilon, V)$  were calculated using the Vienna ab initio simulation package (VASP) [17]. The 0-K calculations were performed in a wide volume range with a step of 0.1 a.u. in the lattice parameter.

At a given temperature  $T$ , the  $F_{\text{ph}}$  in Eq. (2) was calculated in the same lattice parameter step as the 0-K calculations. The phonon energy  $E_{\text{ph}}$  and the phonon heat capacity  $C_{\text{ph},V}$  were derived using the same analytical formula used by Xie et al. [5].  $E_{\text{el}}$  and  $S_{\text{el}}$  were evaluated using one-dimensional integrations as shown in Eqs. (3) and (4).

To calculate the thermal expansion, our strategy is different from that of Xie et al. [5]. We did not calculate the Grüneisen parameter, which is numerically not always stable since a further derivative of  $\omega_j(\mathbf{q}, V)$  against  $V$  must be evaluated. Instead, at any given  $T$ , we calculated the Helmholtz free-energy  $F(V, T)$  as a function of lattice parameter with a step of 0.1 a.u. We then employed the cubic spline interpolation to find the minima of  $F(V, T)$  as a function of  $V$ . We will show in the following sections that this approach is more efficient, stable, and accurate.

## 4. Results and discussions

### 4.1. Bulk properties

The three most frequently examined thermodynamic properties in an ab initio calculation are equilibrium atomic volume ( $V_0$ ), isothermal bulk modulus ( $B_T$ ), and the linear thermal expansion coefficient ( $\alpha$ ) under ambient conditions (i.e.,  $T = 298$  K and pressure  $P = 0$  GPa). The present results for Al (fcc), Ni (fcc), NiAl (B2), and Ni<sub>3</sub>Al (L1<sub>2</sub>) together with the available experimental values are shown in Table 1.

For Ni<sub>3</sub>Al, our calculated  $V_0$  agrees with the experimental data by Kamara et al. [18] up to the fourth digit. For the other cases, the calculated values of  $V_0$  are within 1.4% error from the experimental values. We numerically obtained the bulk modulus  $B_T$  according to the formula,  $B_T = -1/V \partial^2 F / \partial V^2$  and the errors in

Table 1  
Properties of Al (fcc), Ni (fcc), NiAl (B2), and Ni<sub>3</sub>Al (L<sub>1</sub><sub>2</sub>) at ambient conditions

	$V_0$ (Å <sup>3</sup> /atom)		$B_T$ (GPa)		$\alpha$ (10 <sup>-6</sup> /K)	
	Theory	Experiment	Theory	Experiment	Theory	Experiment
Al	16.82	16.60 [19]	68.06	72.2 [20]	24.88	23.1 [21]
Ni	11.09	10.94 [19]	191.6	186 [20]	12.68	13.1 [22]
NiAl	12.16	12.02 [23]	153.5	156 [23]	14.06	11.9 [21]
Ni <sub>3</sub> Al	11.32	11.32 [18]	182.4	N/A	12.17	12.3 [21]

comparison with experimental data are 5.7%, 3.0%, and 1.6% for Al, Ni, and NiAl, respectively. For Ni<sub>3</sub>Al, we did not find the experimental value. The values of  $\alpha$  will be discussed Section 4.3.

4.2. Phonon dispersion

Experimentally, the phonon frequency can be measured directly by inelastic neutron scattering [24–26] or inelastic X-ray scattering [27]. To validate an ab initio calculation, perhaps the most important and interesting step is to calculate the phonon dispersion. Considering that the equilibrium atomic volumes for Al, Ni, and NiAl are overestimated, our calculations were performed at both the theoretical and the experimental atomic volumes. The results are compared with the inelastic neutron scattering measurements [25,26,28] in Figs. 1–4 along the high symmetry lines in the Brillouin zone (BZ). The calculated phonon frequencies with the theoretical  $V_0$  are slightly lower than those of the experiments while the calculations with the experimental  $V_0$  have better agreements with the experiments.

For Al, two previous calculations [8,29] using the local density approximation (LDA) were carried out at the theoretical volume which was smaller than the measured one by about 5%. It appeared the phonon

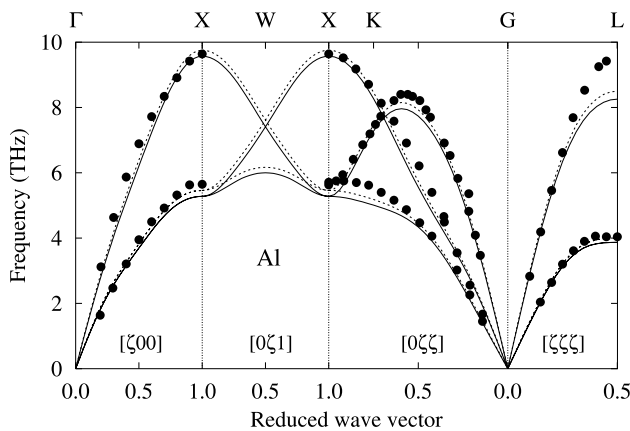


Fig. 1. Phonon dispersion curves of Al. The calculated values at the theoretical volume are plotted as solid lines and the calculated values at the experimental volume are plotted as dashed lines. The data from the inelastic neutron scattering measurement [28] are plotted as solid circles.

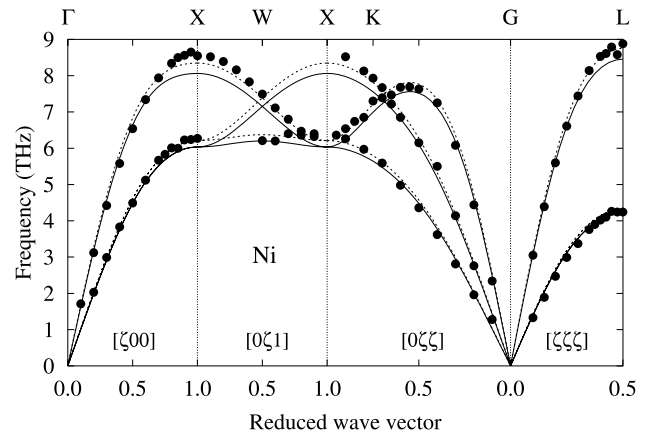


Fig. 2. Phonon dispersion curves of Ni. The calculated values at the theoretical volume are plotted as solid lines and the calculated values at the experimental volume are plotted as dashed lines. The data from the inelastic neutron scattering measurement [28] are plotted as solid circles.

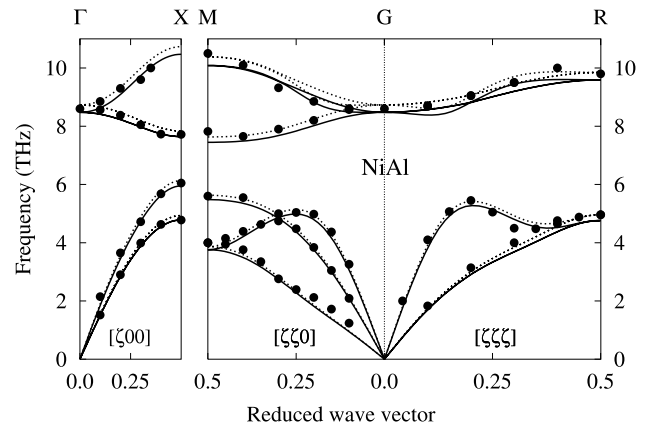


Fig. 3. Phonon dispersion curves of NiAl. The calculated values at the theoretical volume are plotted as solid lines and the calculated values at the experimental volume are plotted as dashed lines. The data from the inelastic neutron scattering measurement [25] are plotted as solid circles.

dispersions derived by de Gironcoli [29] had perfect agreement with the experiment while those by Debernardi et al. [8] shown slightly higher frequencies than the experiment. At the L point, our calculated longitudinal frequencies show the largest deviations from the

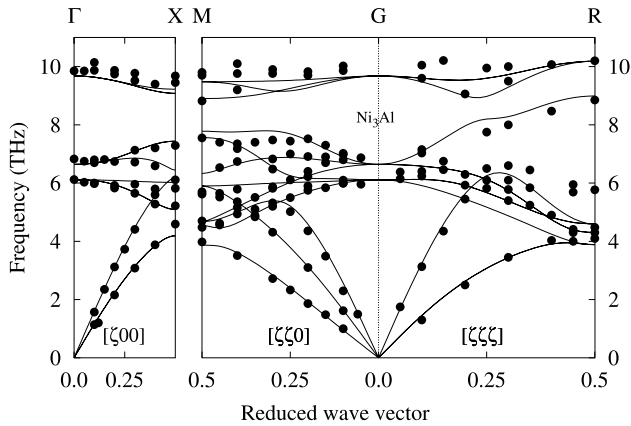


Fig. 4. Phonon dispersion curves of  $\text{Ni}_3\text{Al}$ . The calculated values are plotted as solid lines and those from the inelastic neutron scattering measurement [26] are plotted as solid circles.

experiment among our results. This could be improved by increasing the number of sampling points in the BZ as already noticed by de Gironcoli [29]. As the present work is focused on the thermodynamic properties, the present overall agreements with the experimental data are acceptable.

For Ni, Xie et al. [6] published the calculated phonon dispersions using GGA on high pressures. Our results shown in Fig. 2 are in good agreements with the experiments.

For NiAl, the agreement between our results and the experiment is excellent as plotted in Fig. 3.

For  $\text{Ni}_3\text{Al}$ , van de Walle et al. [3] presented the phonon density of state (calculated using LDA) in their paper. There were also two other published works [7,9] employing the embedded-atom method (EAM) potentials. The EAM phonon frequencies show very large deviations from the experiment for the optical branch. Our results are shown in Fig. 4. At the R point, the phonon frequencies around 5.8 THz were poorly reproduced. The reason could be similar to the case for Al at the L point. Again, the present overall agreement with the experimental data is acceptable since we are more concerned with the thermodynamic properties.

#### 4.3. Thermal expansion

The calculated linear thermal expansion coefficients at zero pressure, with and without considering the thermal electronic contributions, are plotted in Figs. 5–8 together with the assessed data [21,22] from the experiments.

The thermal expansion data of Al assessed by Touloukian et al. [21] are often quoted in the literatures. For Ni, newly recommended data were given by Ho [22]. These two sets of data are sufficiently accurate to be viewed as the experimental standard for comparisons. The calculated  $\alpha$  of Al is higher than that of Touloukian

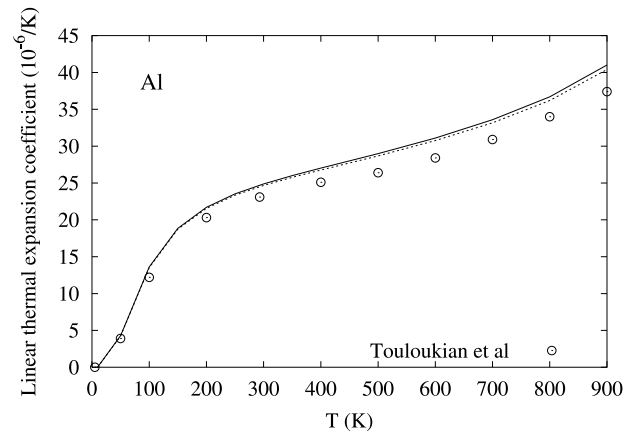


Fig. 5. Linear thermal expansion coefficient of Al. The calculated results, with and without considering the thermal electronic contribution, are plotted as solid and dashed lines, respectively. The data from assessment by Touloukian et al. [21] are plotted as open circles.

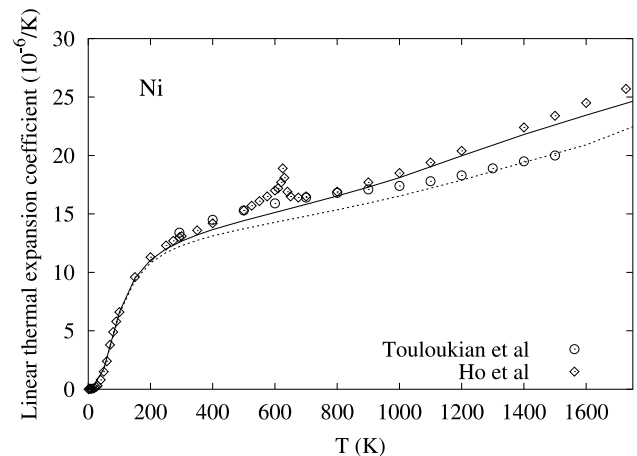


Fig. 6. Linear thermal expansion coefficient of Ni. The calculated results, with and without considering the thermal electronic contribution, are plotted as solid and dashed lines, respectively. The recommended values by Touloukian et al. [21] are plotted as open circles and the newly recommended values by Ho [22] are plotted as open diamonds.

et al. [21] by 10% at 900 K. For Ni, the calculated  $\alpha$ s including TEC are in excellent agreement with the newly recommended values by Ho [22] except a few points near the magnetic transition temperature. TEC is weak for Al as shown by its small coefficient of electronic specific heat  $\gamma = 1.35 \text{ mJ/mol/K}^2$  [20]. In contrast, for Ni the consideration of the thermal electrons increases the thermal expansion coefficient by 10% at the highest temperature studied here.

For NiAl and  $\text{Ni}_3\text{Al}$  alloys, as shown in Figs. 7 and 8, the agreements between the calculations and the recommended data appeared not as good as in the cases of Al and Ni. It should be noted that the values recommended by Touloukian et al. [21] seemed to have larger uncertainties due to the limited experimental data.

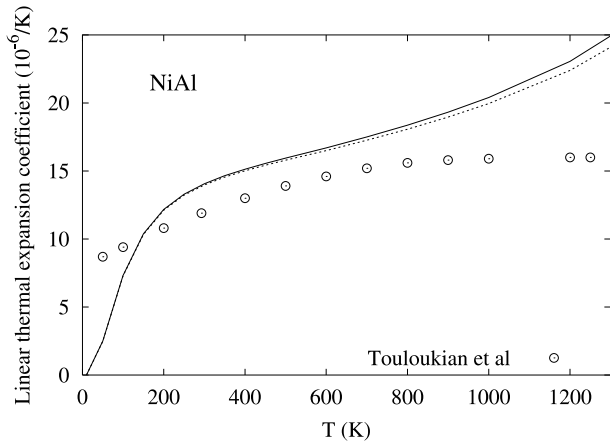


Fig. 7. Linear thermal expansion coefficient of NiAl. The calculated results, with and without considering the thermal electronic contribution, are plotted as solid and dashed lines, respectively. The data by Touloukian et al. [21] are plotted as open circles.

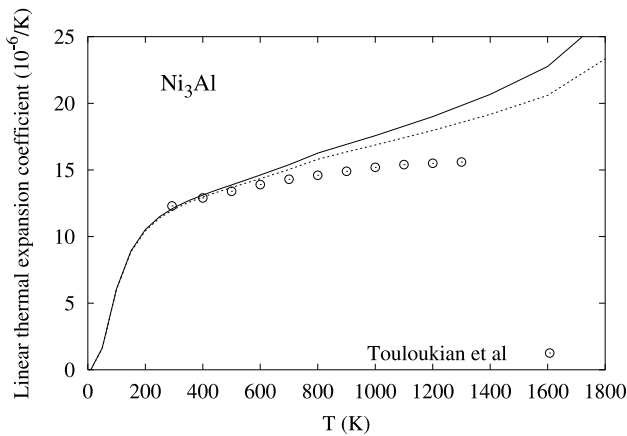


Fig. 8. Linear thermal expansion coefficient of Ni<sub>3</sub>Al. The calculated results, with and without considering the thermal electronic contribution, are plotted as solid and dashed lines, respectively. The data by Touloukian et al. [21] are plotted as open circles.

For example, the recent high-temperature X-ray diffractometry [30] reported an averaged  $\alpha$  of  $17.3 \times 10^{-6}/\text{K}$  between 300 and 1000 K for Ni<sub>3</sub>Al. For these two compounds, the thermal electronic contribution to the  $\alpha$ s for Ni<sub>3</sub>Al is larger than for NiAl. This can be explained by the fact that the electronic DOS (not shown) at the Fermi level for Ni<sub>3</sub>Al are higher than for NiAl.

#### 4.4. Enthalpy as a function of temperature

The enthalpy as a function of temperature is an important thermodynamic quantity in thermodynamic modeling [31–33]. The calculated results at the zero pressure are compared with the other data source in Figs. 9–12. Similar to the case of thermal expansions as discussed in the last section, only experimental results [34,35] of pure metals are reliable. For the compounds,

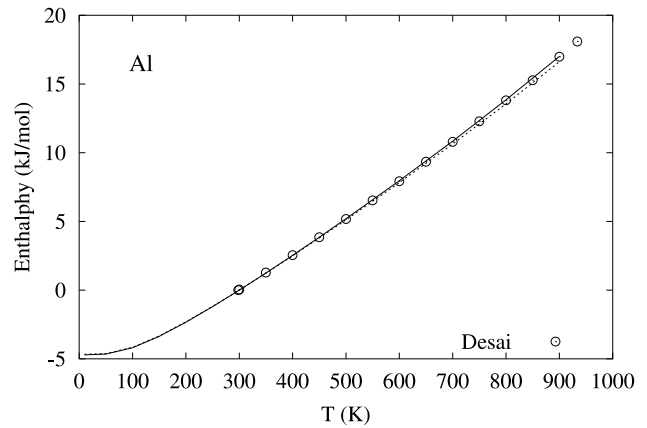


Fig. 9. Enthalpy of Al. The calculated results, with and without considering the thermal electronic contribution, are plotted as solid and dashed lines, respectively. The well-assessed values by Desai [35] are plotted as open circles.

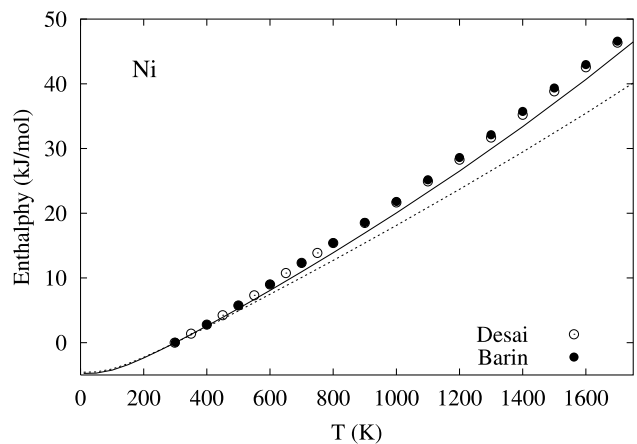


Fig. 10. Enthalpy of Ni. The calculated results, with and without considering the thermal electronic contribution, are plotted as solid and dashed lines, respectively. The well-assessed values by Desai [34] are plotted as open circles, and those recommended by Barin [36] are plotted as solid circles.

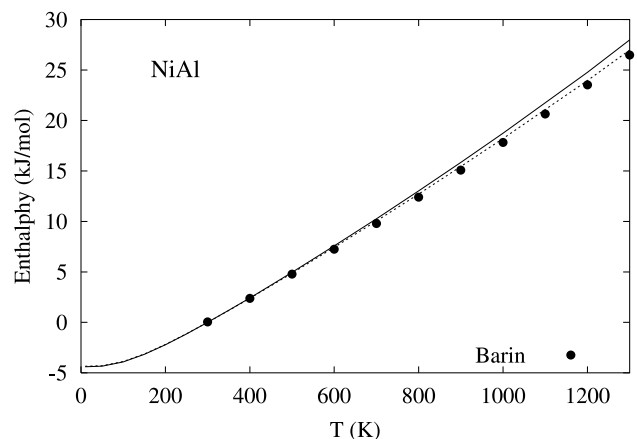


Fig. 11. Enthalpy of NiAl. The calculated results, with and without considering the thermal electronic contribution, are plotted as solid and dashed lines, respectively. The data recommended by Barin [36] are plotted as solid circles.

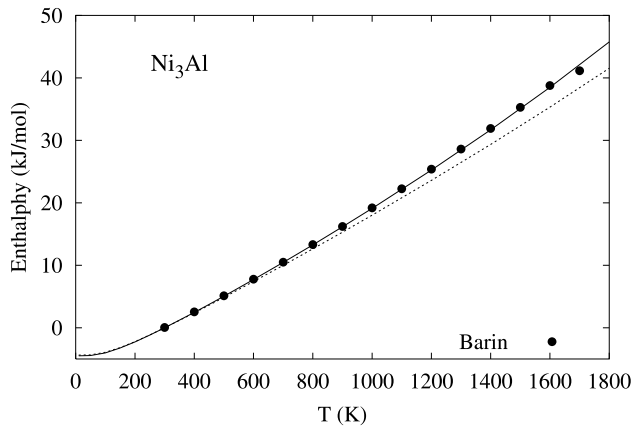


Fig. 12. Enthalpy of  $\text{Ni}_3\text{Al}$ . The calculated results, with and without considering the thermal electronic contribution, are plotted as solid and dashed lines, respectively. The data recommended by Barin [36] are plotted as solid circles.

the recommended values of Barin [36] are shown in Figs. 11 and 12.

Our calculated enthalpy as a function of temperature for Al is almost identical to the recommended value by Desai [35] as shown in Figs. 9. The thermal electronic contribution to enthalpy is weak for Al. For Ni, the agreement between the calculation and the experiment could have been improved further if the effect of magnetic transition occurred at  $\sim 600$  K had been accounted for (Fig. 10). Unfortunately, we do not have a simple way to include the magnetic effect theoretically right now. An important effect for Ni, as we already stated in the theoretical section, is that the thermal electrons can contribute 15% to the enthalpy at 1600 K.

The results for NiAl are shown in Fig. 11. The calculated enthalpy without considering TEC was in better agreement with the recommended values by Barin [36] while those calculated values with considering TEC is about 4% higher at 1300 K.

For  $\text{Ni}_3\text{Al}$ , the calculated enthalpy with considering TEC is again identical to the recommended values by Barin [36] as can be seen in Fig. 12. In this case, the TEC to enthalpy is about 8% at 1600 K.

#### 4.5. Enthalpy of formation as a function of temperature

The enthalpy of formation is more important in evaluating the phase diagram through the thermodynamic modeling [37,38]. Due to the difficulties in making the pure example and the other technical limitation, the experimental results are rather scattered. The measured enthalpies of formation of NiAl are in the range of  $-58.8$  to  $-72$  kJ/mol. For  $\text{Ni}_3\text{Al}$ , they are in the range of  $-37.6$  to  $-47$  kJ/mol. Theoretically, a number of calculations have been carried out (see [39,40]). However, almost all of them are done at 0 K.

We have calculated the enthalpies of formation for NiAl and  $\text{Ni}_3\text{Al}$  as a function of temperature. The

results are compared with experiments (see [39,40], and references therein) in Figs. 13 and 14 for NiAl and  $\text{Ni}_3\text{Al}$ , respectively. The experiments [39,40] show a negative slope against temperature for both NiAl and  $\text{Ni}_3\text{Al}$ . It is fascinating to note that our calculation reproduced this temperature behavior.

At room temperature, our calculated enthalpy of formation for NiAl is  $-62.7$  kJ/mol which is 5% higher than the recently calorimetric value of  $-66.1$  kJ/mol by Rzyman et al. [40]. For  $\text{Ni}_3\text{Al}$ , our calculated enthalpy of formation at 300 K is  $-41.1$  kJ/mol which is extremely close to the calorimetric value of  $-41.3$  kJ/mol by Rzyman et al. [39].

The thermal electronic effects are usually neglected in CALPHAD modeling [37,38] due to a lack of data. Another reason is that in CALPHAD, the enthalpy of

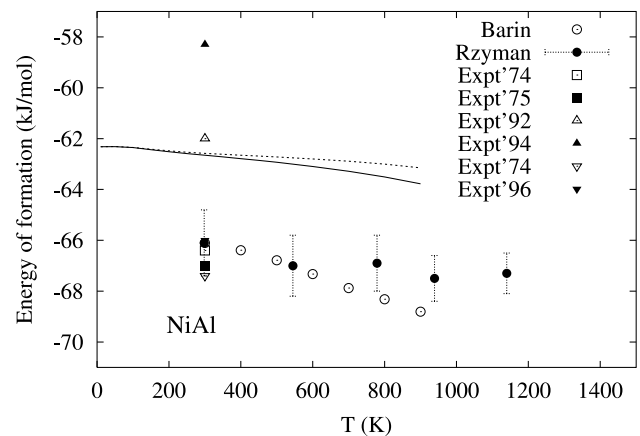


Fig. 13. Enthalpy of formation of NiAl as a function of temperature. The calculated results, with and without the thermal electronic contribution, are plotted as solid and dashed lines, respectively. For other data,  $\circ$ : recommended by Barin [36];  $\bullet$ : measured by Rzyman et al. [40];  $\square$ ,  $\blacksquare$ ,  $\triangle$ ,  $\blacktriangle$ ,  $\nabla$ , and  $\blacktriangledown$ : other measured data, see [40].

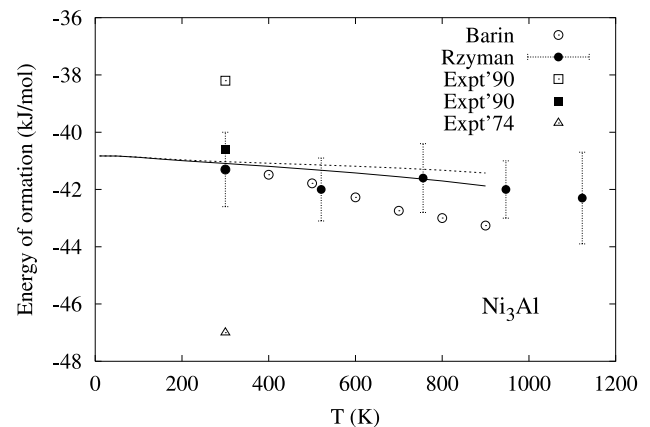


Fig. 14. Enthalpy of formation of  $\text{Ni}_3\text{Al}$  as a function of temperature. The calculated results, with and without the thermal electronic contribution, are plotted as solid and dashed lines, respectively. For other data,  $\circ$ : recommended by Barin [36];  $\bullet$ : measured by Rzyman et al. [39];  $\square$ ,  $\blacksquare$ , and  $\triangle$ : other measured data, see [39].

formation is the more important input than the enthalpy itself for a compound. For the cases of NiAl and Ni<sub>3</sub>Al, our finding is that, after the consideration of the thermal electronic effect, the calculated enthalpies of formation are more temperature dependent. Take Ni<sub>3</sub>Al as an example, the slopes of enthalpy of formation against the temperature are  $-1.2$  and  $-0.67$  J/mol/K, respectively, with and without considering TEC.

## 5. Summary

The ab initio linear-response theory was employed to calculate the phonon dispersions of Al, Ni, NiAl, and Ni<sub>3</sub>Al as a function of atomic volume using the PWSCF method with the Vanderbilt ultra-soft pseudopotential and the generalized gradient approximation. With the derived Helmholtz free-energy, the linear thermal expansions and enthalpies of Al, Ni, NiAl, and Ni<sub>3</sub>Al are obtained. In the present work, the consideration of thermal electronic contribution to the free energy, which is usually neglected in the literature, improves the agreement between the calculations and experiments. The calculated room temperature equilibrium volumes are within 1.4% error from the experimental values. The calculated bulk moduli are within the experiments by 5.7%, 3.0%, and 1.6% for Al, Ni, and NiAl, respectively. Our calculations show that the enthalpies of formation are slightly temperature dependent with a slope of  $-1.6$  J/mol/K for NiAl and  $-1.2$  J/mol/K for Ni<sub>3</sub>Al.

## Acknowledgements

Calculations have been done using the PWscf package [11]. This work is supported by the NASA UEET program under Grant No. NCC3-920. The authors thank Dr. Jorge Sofó for his valuable help and advice. Calculations were carried out on the IBM-SP3 supported by the DOD High Performance Computer Modernization Program at the ASC-MSRC, and the LION-XL cluster at the Pennsylvania State University supported in part by the NSF Grants (DMR-0205232, DMR-9983532 and DMR-0122638) and in part by the Materials Simulation Center at the Pennsylvania State University.

## References

- [1] Baroni S, de Gironcoli S, Dal Corso A, Giannozzi P. *Rev Mod Phys* 2001;73:515.
- [2] van de Walle A, Ceder G. *Rev Mod Phys* 2002;74:11.
- [3] van de Walle A, Ceder G, Waghmare UV. *Phys Rev Lett* 1998;80:4911.
- [4] Li ZQ, Tse JS. *Phys Rev Lett* 2000;85:5130.
- [5] Xie JJ, de Gironcoli S, Baroni S, Scheffler M. *Phys Rev B* 1999;59:965.
- [6] Xie JJ, Chen SP, Brand HV, Rabie RL. *J Phys Condes Matter* 2000;12:8953.
- [7] Ravelo R, Aguilar J, Baskes M, Angelo JE, Fultz B, Holian BL. *Phys Rev B* 1998;57:862.
- [8] Debernardi A, Alouani M, Dreysse H. *Phys Rev B* 2001;63:064305.
- [9] Althoff JD, Morgan D, deFontaine D, Asta M, Foiles SM, Johnson DD. *Phys Rev B* 1997;56:R5705.
- [10] Althoff JD, Morgan D, de Fontaine D, Asta MD, Foiles SM, Johnson DD. *Comput Mater Sci* 1998;10:411.
- [11] Baroni S, Dal Corso A, de Gironcoli S, Giannozzi P. Available from: <http://www.pwscf.org>.
- [12] Landau LD, Lifshitz EM. *Statistical physics*. Oxford, New York: Pergamon Press; 1980–81.
- [13] Nash P, Singleton MF, Murray JL. In: Nash P, editor. *Phase diagrams of binary nickel alloys*. Materials Park, OH: ASM International; 1991.
- [14] Vanderbilt D. Available from: <http://www.physics.rutgers.edu/~dhv/uspp/index.html>.
- [15] Hansen LB. Available from: <http://www.fysik.dtu.dk/CAMPOS/Documentation/Dacapo/PseudoPotentialOverView/>.
- [16] Perdew JP, Wang Y. *Phys Rev B* 1992;45:13244.
- [17] Kresse G, Joubert D. *Phys Rev B* 1999;59:1758.
- [18] Kamara AB, Ardell AJ, Wagner CNJ. *Metall Mater Trans A* 1996;27:2888.
- [19] Available from: <http://www.webelements.com/>.
- [20] Kittel C. *Introduction to solid state physics*. New York: Wiley; 1996.
- [21] Touloukian YS, Kirby RK, Taylor RE, Desai PD. *Thermophysical properties of matter thermal expansion*. New York: Plenum Press; 1975.
- [22] Ho CY. *Properties of selected ferrous alloying elements*. New York, Washington, Philadelphia, London: Hemisphere Publishing Corporation; 1989.
- [23] Otto JW, Vassiliou JK, Frommeyer G. *J Mater Res* 1997;12:3106.
- [24] Fultz B, Anthony L, Nagel LJ, Nicklow RM, Spooner S. *Phys Rev B* 1995;52:3315.
- [25] Mostoller M, Nicklow RM, Zehner DM, Lui SC, Mundenar JM, Plummer EW. *Phys Rev B* 1989;40:2856.
- [26] Statassis C, Kayser FX, Loong C-K, Rach D. *Phys Rev B* 1981;24:3048.
- [27] Manley ME, Lander GH, Sinn H, Alatas A, Hulth WL, McQueeney RJ, et al. *Phys Rev B* 2003;67:052302.
- [28] Dederichs PH, Schober H, Sellmyer DJ. *Phonon states of elements. Electron states and fermi surfaces of alloys*. Berlin, Heidelberg: Springer; 1981.
- [29] de Gironcoli S. *Phys Rev B* 1995;51:6773.
- [30] Nathal MV, Mackay RA, Garlick RG. *Mater Sci Eng* 1985;75:195.
- [31] Huang W, Chang YA. *Intermetallics* 1998;6:487.
- [32] Huang W, Chang YA. *Intermetallics* 1999;7:625.
- [33] Ansara I, Dupin N, Lukas HL, Sundman B. *J Alloy Comp* 1997;247:20.
- [34] Desai PD. *Int J Thermophys* 1987;8:763.
- [35] Desai PD. *Int J Thermophys* 1987;8:621.
- [36] Barin I. *Thermochemical data of pure substances*. New York, Basel, Cambridge, Tokyo: Weinheim; 1995.
- [37] Kaufman L, Bernstein H. *Computer calculation of phase diagram*. New York: Academic Press; 1970.
- [38] Saunders NP. *MA CALPHAD (calculation of phase diagrams): a comprehensive guide*. Oxford, New York: Pergamon Press; 1998.
- [39] Rzyman K, Moser Z, Watson RE, Weinert M. *J Phase Equilib* 1996;17:173.
- [40] Rzyman K, Moser Z, Watson RE, Weinert M. *J Phase Equilib* 1998;19:106.